

# Electrical conductivity of metal–carbon nanotube structures: Effect of length and doping

R NIGAM<sup>1\*</sup>, S HABEEB<sup>2</sup>, A PRIYADARSHI<sup>3</sup> and N JAGGI<sup>1</sup>

<sup>1</sup>Department of Physics, National Institute of Technology, Kurukshetra 136 119, India

<sup>2</sup>Department of Physics, Jamia Millia Islamia, New Delhi 110 025, India

<sup>3</sup>Carlsys Technologies Private Limited, New Delhi 110 092, India

MS received 17 December 2012; revised 18 February 2013

**Abstract.** The electrical properties of asymmetric metal–carbon nanotube (CNT) structures have been studied using density functional theory and non-equilibrium Green's function method with Atomistix tool kit. The models with asymmetric metal contacts and carbon nanotube bear resemblance to experimental set-ups. The study shows the effect of varying length of carbon nanotube on electronic transmission and conductance of various structures. The effects of silicon doping on CNT-based structures have also been studied. The conductance of structure with longer CNT is more compared with shorter CNT. Silicon doping increases the conductivity of carbon nanotube-based structure.

**Keywords.** Density functional theory; non-equilibrium green function; carbon nanotube; silicon; conductance.

## 1. Introduction

Carbon nanotubes (CNTs) are unique nanomaterials finding use in various applications due to their high electrical conductivity, efficient thermal conductivity and extraordinary mechanical strength. The electrical properties of CNTs depend on their geometrical structure (Saito *et al* 1992). CNTs can be metallic, semi-metallic or semi-conducting with different energy band gaps depending on diameter and the indices ( $n$ ,  $m$ ). Armchair ( $n$ ,  $n$ ) tubes are always metallic and ( $n$ ,  $m$ ) tubes (with  $n - m = 3j$ ; where  $j$  is a non-zero integer) are semi-metallic, whereas all other tubes are large gap semiconductors. The extraordinary characteristics of CNTs give them the potential to be used in materials science, electronics, biomedical, energy management and many other fields. Semiconducting carbon nanotubes find their use in the formation of transistors (Tans 1998; Weitz *et al* 2007), diodes (Yang *et al* 2005; Lu *et al* 2006), sensors (Meng *et al* 2007; Wang and Hu 2012) and non-volatile memory devices (Durkop *et al* 2004; Jeong and Jiang 2007).

Currently, lot of research is going on in the area of asymmetric metal–CNT contact-based structures. They may have wide applications in high frequency devices due to their high charge carrier mobility, high current transport capability and low capacitances (Dresselhaus *et al* 2001). Recently, devices such as CNT Schottky diodes have been fabricated, modelled and studied (Bai

*et al* 2008). The rectification behaviour of Schottky diode depends upon work function of contact metal and characteristics of interface (Tung 2001). However, there is a lack of understanding of the metal–CNT contact interface despite extensive studies, because the exact geometry of atoms at interface is not known during experiments. In this work, we have tried to study the change in the electrical conductivity of structures with asymmetrical metal–CNT contacts by changing the length of CNT. We also investigate the effect of CNT with strong quantum confinement effect in these structures as strong hybridization effects occur in small radius nanotubes which significantly alter their electronic structure (Miyake and Saito 2003).

Doping of CNTs with silicon, boron or nitrogen modifies the electronic properties and the structure significantly from pristine CNTs (Song *et al* 2006; Jiang *et al* 2007; Nxumalo and Coville 2010). Silicon and carbon lie in the same column in the periodic table, but silicon has  $sp^3$  bonding as compared to carbon which prefers  $sp^2$  bonding. This may lead to changes in the electronic properties of CNTs. We have studied the changes in electrical conductivity of asymmetric metal–CNT contact-based structures, when CNT is substitutionally doped with silicon atoms.

## 2. Modelling approach

We have built atomic models for the analysis of current–voltage ( $I$ – $V$ ) characteristics and transmission spectrum

\*Author for correspondence (ravinigam09@gmail.com)

of the asymmetrical metal–pristine CNT and silicon-doped CNT structures with reference to experimental set-ups (Yang *et al* 2005; Lu *et al* 2006). A two probe system consists of a central scattering region comprising structures to be analysed and semi-infinite left and right electrodes. The gold atoms have been used to make bulk electrodes. The gold electrodes provide ohmic contact and the effect of electrodes can be corrected through self-energy (Datta 2000). A model with CNT (4, 0) partially embedded with aluminium atoms has been built. For our model CNT (4, 0) has been taken, because it has a strong quantum confinement effect and is expected to be stable in a free space (Mohammadzadeh 2006). Aluminium has been used because it has low work function which leads to formation of a junction barrier.

The configuration of our final model, i.e. central scattering region, when observed, consists of 7 aluminium and 16 carbon atoms of CNT. The total length of central scattering region is 11.96 Å (figure 1). The yellow sphere represents the atoms of bulk gold electrodes. The central scattering region is represented by grey spheres symbolizing carbon nanotube partially embedded by aluminium atoms denoted by purple spheres.

Substitutional silicon doping is done in the same model to form a new asymmetric metal–silicon-doped CNT model (figure 2). The yellow sphere represents the atoms of bulk gold electrode. The central scattering region is represented by grey spheres symbolizing carbon nanotube partially embedded by aluminium atoms as denoted by

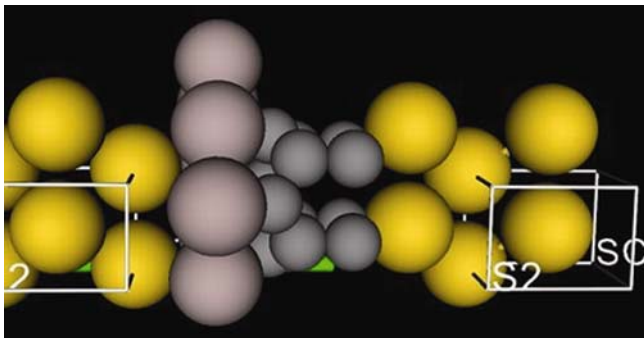


**Figure 1.** Asymmetric metal–CNT structure with central scattering region of length 11.96 Å.

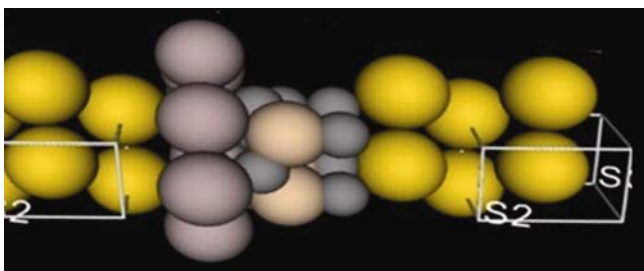


**Figure 2.** Asymmetric metal–silicon-doped CNT structure.

purple spheres. Doped silicon atoms are represented by orange spheres. Three atoms of carbon from central scattering region have been substituted by silicon. The framework of the model consists of 7 aluminium, 13 carbon and 3 silicon atoms.

The third model is made by increasing the length of the CNT (4, 0). The third model is a longer version of the first model. The length of central scattering region has been increased from 11.96 to 17.32 Å (figure 3). The sticks represent the chemical bonds.

The structural optimizations were performed by using a conjugated gradient procedure for minimization of the total energy with analytic forces from DFT (Sugino and Oshiyama 1992). The structural relaxation leads to slight deformation of CNT in the radial direction. The distance between the nearest aluminium and carbon atoms in a different plane ranges between 1.98 and 2.14 Å. The electronic transport properties of each model are studied by using density functional theory (DFT) and non-equilibrium Green's function (NEGF) first principles method within the Landauer formalism implemented in Atomistix tool kit (Brandbyge *et al* 2002). DFT with Perdew–Burke–Ernzerhof exchange correlation functional within the generalized gradient approximation and NEGF are used to deal with atomic structure self-consistently under non-equilibrium conditions. We used the double zeta polarized basis set for valence wave functions and core electrons of all the atoms are described by norm-conserving Troullier–Martins pseudopotentials (Troullier and Martins 1991). The mesh cut off was set at 150 Rydberg for the system.

### 3. Theory

The electronic and transport properties of nanoscale system can be studied using self-consistent DFT–NEGF method which utilizes the solution of standard Kohn–Sham equations (Sankey and Niklewski 1989; Sorensen *et al* 2009). The left and right semi-infinite electrodes are represented by Kohn–Sham Green's functions,  $G_L$  and  $G_R$ . The central scattering region is described by a Kohn–Sham equation (where the coupling to the electrodes is incorporated with

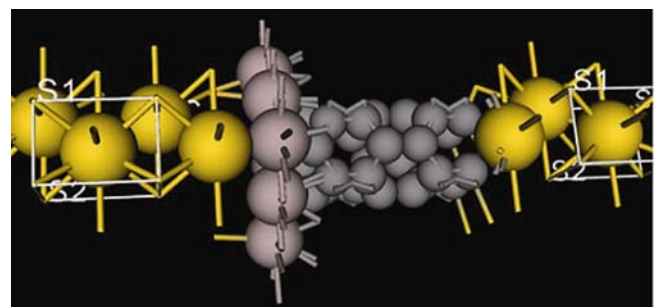


**Figure 3.** Asymmetric metal–CNT structure with central scattering region of length 17.32 Å.

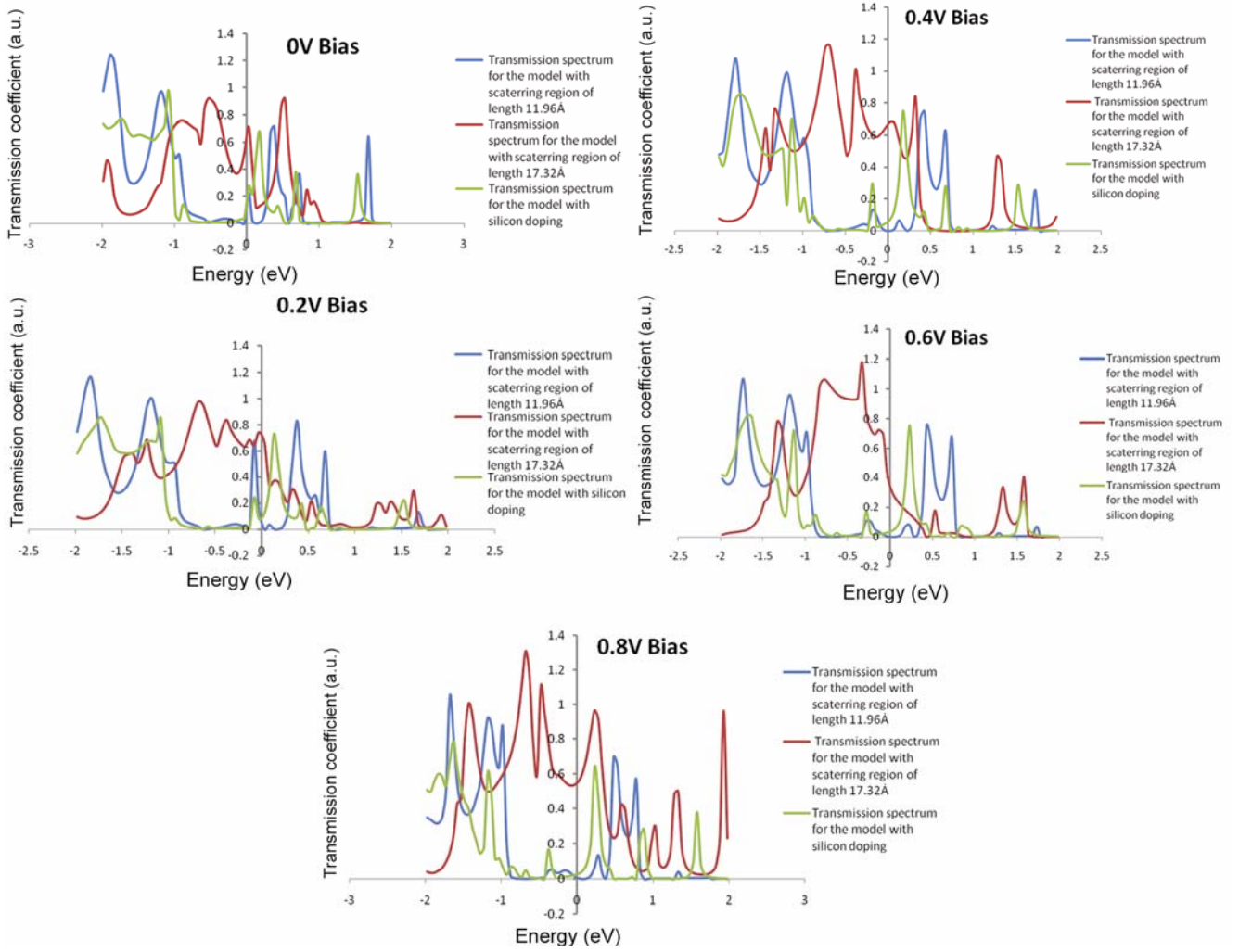


**Figure 4.** Transmission spectra for the three models at different bias voltages.

Kohn–Sham effective potential by non-Hermitian self-energy operators), thus

$$\Sigma_L = H_{CL}G_LH_{LC}, \quad \Sigma_R = H_{CR}G_RH_{RC}, \quad (1)$$

where  $H_{CL}$ ,  $H_{LC}$ ,  $H_{CR}$ ,  $H_{RC}$  are the blocks of Kohn–Sham–Hamiltonian matrix connecting the central region with left/right electrodes.

The Green’s function gives the response of a system to the constant perturbation in the Schrodinger equation.

Green function of the complete system is

$$G = (ES - H - \Sigma_L - \Sigma_R)^{-1}, \quad (2)$$

where  $S$  is the overlapping matrix which would be equal to the identity matrix for orthogonal basis states. Overlapping matrix arises due to non-orthogonality of the pseudo-atomic orbitals.

Transmission probability in the transmission matrix,  $T_R()$  form is

$$T(E) = T_R((\Sigma_L - \Sigma_L^+)G(\Sigma_R^+ - \Sigma_R)G^+), \quad (3)$$

where  $\Sigma_{L/R}$  are the self-energy terms of left/right electrodes.

Using non-equilibrium Green function formalism, the current through the system can be obtained from the transmission function,  $T(E)$ , using Landauer–Buttiker formula (Buttiker *et al* 1985)

$$I(V) = 2e/h \int_{-\infty}^{\infty} T(E)(f(E, \mu_L) - f(E, \mu_R))dE, \quad (4)$$

where  $f$  denotes Fermi distribution function at room temperature with electrochemical potential  $\mu_{L/R} = E_F \pm eV/2$ , referring to the left and right electrodes, respectively.

Differential conductance is the derivative of the current w.r.t. voltage (Tian *et al* 1998)

$$G = 0.5G_o (T(\mu_L) + T(\mu_R)), \quad (5)$$

where  $G_o = 2e^2/h$  (quantum of conductance).

#### 4. Results and discussion

We have analysed the transmission spectrum for the models with central scattering region of length 17.32 and

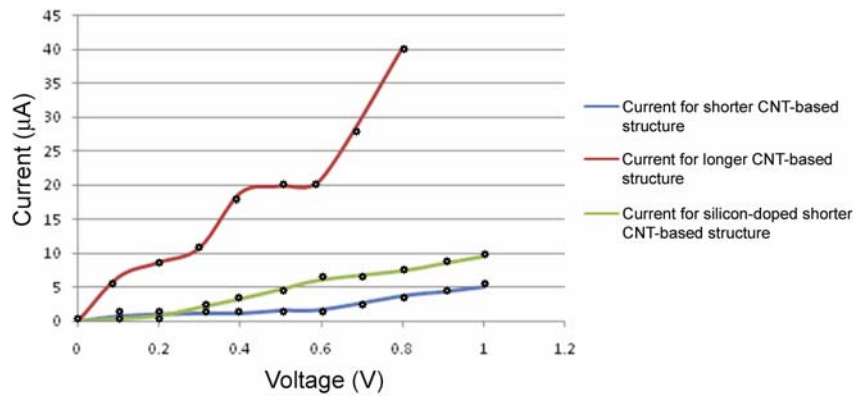


**Figure 5.**  $I$ - $V$  characteristics for three asymmetric metal-CNT models. The dots represent the value of current for respective step-bias voltage.

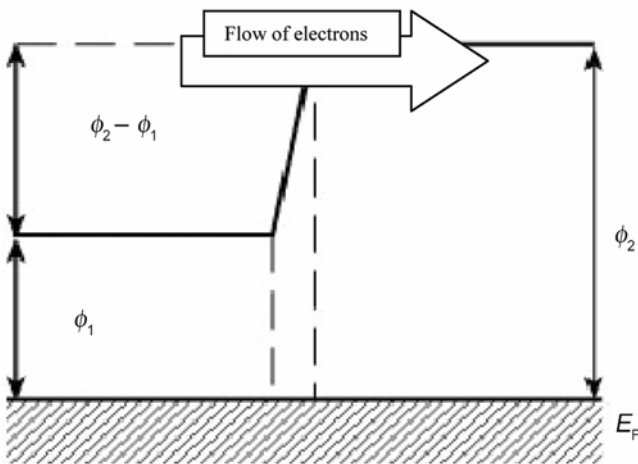


**Figure 6.** Formation of a metal-metal junction.

11.96 Å and for the model with central scattering region constituting silicon-doped CNT (figure 4). The transmission spectra are calculated at various bias voltages represented as  $(-V/2, +V/2)$ , where  $V$  is the applied voltage. The sampling of the bias voltage axis was 0.1 V and individual calculations of current were done for each bias. Fermi level is considered at 0 eV to make the calculations easy.

The transmission coefficients, along with the available states, signify the magnitude of conducting channel. The more the value of transmission coefficient and unoccupied states for a bias voltage, the more are the conducting channels and higher is the value of current. The current for a given bias voltage is obtained by integration procedure involving whole energy range of the transmission spectrum. So, the value of current is proportional to the area under the transmission spectrum and transmission is a magnitude of interest only after integration.

The graph shows the increase in electronic transmission with the increase in voltage in all the three cases. The transmission spectrum for the longer model has

higher value of transmission coefficient for larger energy intervals as compared to shorter models. This leads to more area covered by transmission spectrum of longer CNT-based structure as compared to shorter CNT-based structure. So the increase in the length of model has resulted in the increased flow of electrons through metal-CNT junction leading to an increase in the electrical conductivity as compared to the models with the shorter length. There is a slight increase in the number of conducting channels for silicon-doped CNT-based structure than that for the pristine CNT-based structure.

The  $I$ - $V$  characteristics bear resemblance to ohmic resistive element (figure 5). The graph shows current-voltage characteristics for the three asymmetric metal and carbon nanotube contact-based structures. The red line represents the current for longer CNT-based structure, green line for silicon-doped shorter CNT-based structure and blue line for shorter CNT-based structure at various bias voltages. The ohmic behaviour is due to the fact that CNT (4, 0) has a strong quantum confinement effect. The small radius and strong curvature effect of CNT (4, 0) lead to metallic conductivity nature of CNT as compared to semiconducting nature as predicted by tight-binding model.

This leads to a metal-metal junction between aluminium and CNT (4, 0). Figure 6 depicts the formation of metal-metal junction.  $\phi_1$ ,  $\phi_2$  are the work functions and  $E_F$  is the Fermi level of final system. The height of the potential barrier is  $(\phi_2 - \phi_1)$ . The electrons will flow from material with lower work function to that with higher work function. Electron transfer lasts until Fermi levels are equal on both sides of the junction. This flow of electrons will lead to accumulation of charge at the metal junction leading to the formation of junction barrier. The electric field hence produced will oppose the flow of electrons. The junction width is very small and the current will increase with the increase in voltage as the electron gains energy to cross the barrier leading to ohmic characteristics. However,  $I$ - $V$  characteristics for longer, shorter

and doped scattering regions show deviation from the perfect ohmic nature. The non-ohmic nature may be due to geometry of asymmetric metal–CNT structures as the electronic conductance significantly depends on the metal–CNT interface (Deretzis and Magna 2006).

The current for longer scattering region is greater than for shorter and doped scattering regions. The conductivity of longer CNT-based structure may be attributed to the increase in the density of states with the increasing tube length (Rocheffort *et al* 1999). The increase in the CNT density of state will lead to unoccupied states near the Fermi level. So, there will be an increase in the number of electrons that cross the junction barrier due to the presence of more number of available states. This accounts for the increase in the electrical conductivity of longer CNT model as compared to the models with shorter length.

There is a slightly more increase in the conductivity of silicon-doped CNT-based structure than that of the pristine CNT-based structure. This may be due to the weaker Si–C bonds as compared to C–C bonds and bigger size of silicon atom. The preference of  $sp^3$  hybridization by Si as compared to the carbon atom may alter the electronic characteristics of structures leading to the formation of impurity band above the Fermi level. The changes in the electronic properties may also be attributed to the distortions arising due to the changes in the bonding characteristics of highest occupied molecular orbitals (HOMO) and lowest unoccupied molecular orbitals (LUMO) of the tube when doped with Si atoms (Jose and Datta 2012; Mohan and Datta 2010). This will result in the increased conductivity of doped structures due to more free movement of charge carriers.

## 5. Conclusions

The electrical properties of asymmetric metal–CNT structures and the effect of silicon doping on them have been studied. The electrical conductivity of the structures with asymmetric metal–CNT contact and small central scattering region increases with the increase in length of CNT. The increase in the electrical conductivity with the increase in the length of CNT is a useful property that can be used for future nanoscale device fabrication. The present work further demonstrates that the increase in conductivity of CNT-based structures, when substitutionally doped with silicon atoms. The findings are expected to be helpful in the application of CNTs in nanoelectronic devices and novel solar cells. However, there is a further scope of analysing the energy bands and interface effects for incorporating CNTs in potential devices.

## Acknowledgements

We acknowledge the beneficial discussion with Professor P Pachauri of Noida Institute of Engineering and Technology, Greater Noida, Uttar Pradesh, India.

## References

- Bai P, Li E, Lam K T, Kurniawan O and Koh W S 2008 *Nanotechnology* **19** 115203
- Brandbyge M, Mozos J, Ordejon P, Taylor J and Stokbro K 2002 *Phys. Rev.* **B65** 165401
- Buttiker M, Imry Y, Landauer R and Pinhas S 1985 *Phys. Rev.* **B31** 6207
- Datta S 2000 *Superlatt. Microstruct.* **28** 253
- Deretzis I and Magna A L 2006 *Nanotechnology* **17** 5063
- Dresselhaus M S, Dresselhaus G and Avouris P 2001 *Carbon nanotubes: synthesis, structure, properties and applications* (Berlin: Springer) p. 147
- Durkop T, Getty S A, Cobas E and Fuhrer M S 2004 *Nano Lett.* **4** 35
- Jeong W K and Jiang Q 2007 *Nanotechnology* **18** 095705
- Jiang Q, Qian L, Yi J, Zhu X and Zhao Y 2007 *Fron. Mater. Sci. China* **1** 379
- Jose D and Datta A 2012 *J. Phys. Chem.* **C116** 24639
- Lu C, An L, Fu Q, Liu J, Zhang H and Murduck J 2006 *Appl. Phys. Lett.* **88** 133501
- Meng S, Maragakis P, Papaloukas C and Kaxiras E 2007 *Nano Lett.* **7** 45
- Miyake T and Saito S 2003 *Phys. Rev.* **B68** 155424
- Mohammadzadeh M R 2006 *Physica E* **31** 31
- Mohan V and Datta A 2010 *J. Phys. Chem. Lett.* **1** 136
- Nxumalo E N and Coville N J 2010 *Materials* **3** 2141
- Rocheffort A, Salahub D R and Avouris Ph 1999 *J. Phys. Chem.* **B103** 641
- Saito R, Fujita M, Dresselhaus G and Dresselhaus M S 1992 *Appl. Phys. Lett.* **60** 2204
- Sankey O F and Niklewski D J 1989 *Phys. Rev.* **B40** 3979
- Song C, Xia Y, Zhao M, Liu X, Li F, Huang B, Zhang H and Zhang B 2006 *Phys. Lett.* **A358** 166
- Sorensen H H B, Hansen P C, Petersen D E, Skelboe S and Stokbro K 2009 *Phys. Rev.* **B79** 205322
- Sugino O and Oshiyama A 1992 *Phys. Rev. Lett.* **68** 1858
- Tans S J, Verschueren A R M and Dekker C 1998 *Nature* **393** 49
- Tian W, Datta S, Hong S, Reifengerger R, Henderson J and Kubiak C P 1998 *J. Chem. Phys.* **109** 2874
- Troullier N and Martins J L 1991 *Phys. Rev.* **B43** 1993
- Tung R T 2001 *Phys. Rev.* **B64** 205310
- Wang X N and Hu PA 2012 *Front. Mater. Sci.* **6** 26
- Weitz R T, Zschieschang U, Effenberger F, Klauk H, Burghard M and Kern K 2007 *Nano Lett.* **7** 22
- Yang M H, Teo K B K, Hasko D G and Milne W I 2005 *Appl. Phys. Lett.* **87** 253116